Available online at www.sciencedirect.com
ScienceDirect
Scripta Materialia 59 (2008) 414–417
Scripta MATERIALIA
www.elsevier.com/locate/scriptamat

Glide of hollow fibers at the bridging stage of fracture in ceramic nanocomposites

M.Yu. Gutkin* and I.A. Ovid'ko

Institute of Problems of Mechanical Engineering, Russian Academy of Sciences, Bolshoj 61, Vasilievskii Ostrov, Saint Petersburg 199178, Russia

Received 16 March 2008; revised 10 April 2008; accepted 11 April 2008
Available online 20 April 2008

A dislocation model is proposed which describes the glide of hollow fibers as a mechanism of energy relaxation at the bridging stage of fracture in ceramic nanocomposites. An elementary event of such glide is treated through generation and slip of a prismatic dislocation loop along the fiber–matrix interface. We calculate the critical shear stress necessary for barrier-less loop nucleation and investigate its dependence on the elastic and geometric properties of a fibrous nanocomposite.

Keywords: Nanocomposite; Fracture; Dislocation theory

Ceramic nanocomposites are highly attractive for a wide range of uses in advanced technologies due to their superstrength and superhardness at both room and high temperatures [1–10]. The general deficiency of most of these materials is still their low toughness. However, a fairly high toughness has been shown by several ceramic nanocomposites [1,2,4–6], in particular those reinforced by carbon nanotubes [2,5,6]. These examples have stimulated interest in understanding the micromechanisms which hamper the growth of cracks and are specific for nanostructures. This paper is aimed at the elaboration of a theoretical model describing the glide of hollow fibers (in particular, carbon nanotubes) through generation and glide of nanoscale dislocation loops, providing effective strain energy relaxation near cracks growing in the bridging regime in ceramic nanocomposites.

Consider a model fibrous nanocomposite consisting of ceramic matrix and unidirectional continuous nanoscale fibers (nanotubes). Let a mode-I crack propagate across the fibers in the nanocomposite. At the initial (bridging) stage of the crack propagation, the matrix is cracked while the fibers remain unbroken and bridge the crack borders. Such a bridging regime has been investigated in detail in conventional fibrous ceramic composites [11–15]. In the case of nanocomposites, the bridging regime has specific features due to the nanoscale effects [4]. We assume that the following four steps of this regime occur along with crack opening in nanocomposites: (1) the fibers are stretched inside the crack but do not glide in the fiber–matrix interface; (2) the fibers start to glide through generation of nanoscale prismatic dislocation loops surrounding the fibers and gliding in the interface from the crack surface to the nanocomposite bulk (Fig. 1a); (3) the glide of fibers is developed through emission of new such loops which can be stopped by interface obstacles, thus producing dislocation pile-ups; (4) these pile-ups provide fiber ruptures which propagate by consuming new loops. The fourth step precedes the transition to the pull-out stage of the crack opening when the broken fibers are pulled out the matrix. The above scheme can be realized if the debonding of fibers is prevented at all four steps of the bridging regime. The debonding usually occurs in conventional ceramic composites [14–17]. In nanocomposites, where the fiber diameter ranges from units to tens of nanometers, there is not enough space for an interface crack to reach the Griffith size, and the suggested dislocation mechanism of energy relaxation can be more effective. Its realization is characterized by the conditions necessary for nucleation of the first dislocation loops. To estimate these conditions, let us analyze the following simplified model.

Consider a prismatic circle dislocation loop with Burgers vector $\boldsymbol{b}$ around a hollow fiber (nanotube) with the outer radius a and wall thickness h (Fig. 1a). Let the

* Corresponding author. E-mail: gutkin@def.ipme.ru

1359-6462/$ - see front matter © 2008 Acta Materialia Inc. Published by Elsevier Ltd. All rights reserved.
doi:10.1016/j.scriptamat.2008.04.016

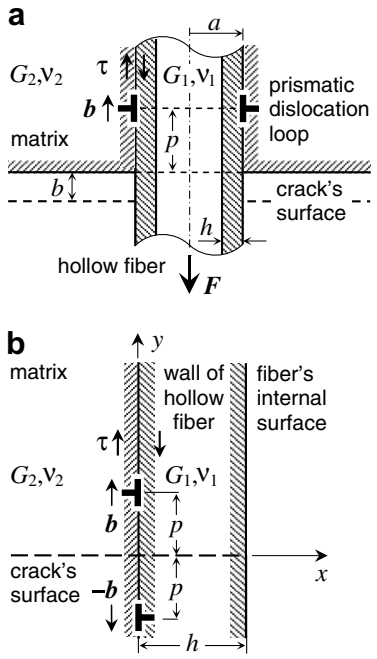

Figure 1. Dislocation model for the glide of a hollow fiber on the matrix–fiber interface near the bridged crack in a fibrous ceramic nanocomposite. (a) Nucleation of a circular prismatic dislocation loop in the interface around the hollow fiber under the local shear stress τ. (b) Simplified model for approximate calculation of the loop strain energy in the limiting case of a thin-wall fiber ($\lambda = h/a \ll 1$): a dipole of straight edge dislocations in the interface between a planar thin layer (fiber wall) and a semi-infinite substrate (matrix).

loop be nucleated at the crack surface and glide from it by the distance p under a local shear stress τ which arises due to the fiber being stretched by the force $\boldsymbol{F}$. For the sake of simplicity, we assume that the fiber and matrix are elastically isotropic and characterized by the shear moduli G_1 and G_2, and the Poisson ratios ν_1 and ν_2, respectively. Since we consider the situation near the point of loop nucleation, we suppose the shear stress τ to be constant. The loop nucleation leads to a change in the system energy that can be written as $\Delta W = W_{\rm el} + W_{\rm c} + \Delta W_{\rm s} - W_\tau$, where $W_{\rm el} = w_{\rm el} 2\pi a$ is the strain energy of the loop, $W_{\rm c} = \overline{D} b^2 Z 2\pi a$ is its core energy, $\Delta W_{\rm s} = (\gamma_1 - \gamma_b) 2\pi a b$ is the surface energy change, and $W_\tau = \tau 2\pi a b p$ is the work done by the stress τ to generate the loop. Here $w_{\rm el}$ is the strain energy of the loop per its unit length, $\overline{D} = (D_1 + D_2)/2$, $D_i = G_i/[\pi(1 + k_i)]$, $k_i = 3 - 4\nu_i$; $i = 1, 2$, $Z \approx 1$, γ_1 and $\gamma_{\rm b}$ are the specific energies of the fiber surface and fiber–matrix interface, respectively. The interface energy $\gamma_{\rm b}$ strongly depends on bonding and misfit across the fiber–matrix interface and can be calculated within a combined atomic-continuum approach [18]. For the purposes of our work, it is enough to take $\gamma_{\rm b}$ as a parameter of the model.

Since correct analytical calculation of $w_{\rm el}$ for the model shown in Figure 1a is hardly possible, we consider only its special case $a \gg h$ which is of practical interest because it is readily applied to the nanocomposites reinforced by nanotubes. In this case, the inside free surface of the fiber is very close to the dislocation line and provides a stronger screening effect on the dislocation elastic fields than the loop shape of the dislocation. Therefore, we can use a greatly simplified planar model (Fig. 1b) to estimate the strain energy $w_{\rm el}$. Now the model system is a straight edge dislocation in the interface between a semi-infinite substrate (matrix) and a thin layer (fiber wall). The dislocation attraction to the crack surface is modeled by an image dislocation with Burgers vector $-\boldsymbol{b}$. As a result, $w_{\rm el}$ is approximated as the strain energy of the dislocation dipole located in the interface of a semi-infinite substrate and a thin layer. Based on the stress fields of an edge dislocation in a thin two-layer plate [18,19], in the limiting case of a semi-infinite substrate we obtain $w_{\rm el}$ as the work done to generate the dislocation dipole in its proper stress field. In doing so, we have

$$w_{\rm el} = D_1 b^2 \left\{ (2 - A - B) \ln \frac{2p - r_{\rm c}}{r_{\rm c}} + 2 \int_0^{+\infty} \sin(sp) \sin[s(p - r_{\rm c})] f(s, h, A, B) \frac{{\rm d}s}{s} \right\}, \quad (1)$$

where $A = (1 - \Gamma)/(1 + k_1\Gamma)$, $B = (k_2 - k_1\Gamma)/(k_2 + \Gamma)$, $\Gamma = G_2/G_1$, $r_{\rm c}$ is the cut-off radius of dislocation stresses on its core, and the function $f(s, h, A, B)$ is

$$f(s,h,A,B) = \frac{{\rm e}^{-4sh}[(1 + AB)(A + B) - 4AB] - 2{\rm e}^{-2sh}[2(1 - A)^2 s^2 h^2 - (1 - A)(2 - A - B)sh + (1 - A)(1 - B)]}{{\rm e}^{-4sh} AB - {\rm e}^{-2sh}(4As^2h^2 + A + B) + 1} \quad (2)$$

The difference $\gamma_1 - \gamma_{\rm b}$ can be rewritten as $\gamma_1(1 - \alpha)$ with $\alpha = \gamma_{\rm b}/\gamma_1$. Using the standard estimate $\gamma_1 \approx G_1 b/8$, one can express the difference through the fiber elastic moduli and ratio α: $\gamma_1 - \gamma_{\rm b} \approx D_1 b\pi(1 - \nu_1)(1 - \alpha)/2$. After some algebra, the energy change $\Delta w = \Delta W/(2\pi a)$ per unit dislocation length reads

$$\frac{\Delta w}{D_1 b^2} = (2 - A - B) \ln(2\xi - 1) + 2 \int_0^{+\infty} \sin(\eta\xi) \sin[\eta(\xi - 1)] f(\eta, \lambda, A, B) \frac{{\rm d}\eta}{\eta} + \frac{1}{2}\left(1 + [\Gamma + \pi(1 - \nu_2)(1 - \alpha)] \frac{1 - \nu_1}{1 - \nu_2}\right) - \frac{\tau}{D_1}\xi, \quad (3)$$

where $\xi = p/b$, $\eta = sb$, $\lambda = h/b$ and $r_{\rm c} \approx b$. The results of numerical calculations of the function $\Delta w(\xi)$ are shown in Figure 2 for the following parameter values: $\Gamma = 0.1$, $\nu_1 = \nu_2 = 0.3$, $\alpha = 0.5$, $\lambda = 5$ and 100 and $\tau/D_1 = 0 \div 1.1$. It is seen that the function $\Delta w(\xi)$ strongly depends on the local stress τ. When τ is small (here $\tau = 0$), the function is positive and grows monotonously, which means that loop generation is impossible.

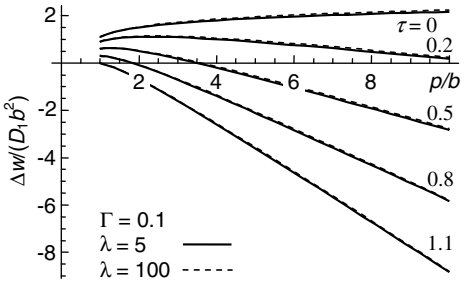

Figure 2. Dependence of the energy change Δw on the normalized dislocation path $\xi = p/b$ at different values of the local shear stress τ for $\Gamma = 0.1$ and $\lambda = 5$ and 100. The energy change is given in units of $D_1 b^2$. The stress values are shown at the curves in units of D_1.

At a larger τ (here $\tau = 0.2D_1$ and $0.5D_1$), $\Delta w(\xi)$ is positive at small ξ and first grows, reaches a maximum and then decreases, becoming negative at large ξ. This means that the loop may be nucleated but must overcome an energy barrier whose height and position depend on τ. When τ is large enough (here $\tau = 0.8D_1$), $\Delta w(\xi)$ is first positive but monotonously decreases and then becomes negative. Therefore, a small energy barrier still exists. At the end, under some critical stress $\tau = \tau_c$ (here $\tau = 1.1D_1$), $\Delta w(\xi)$ is always non-positive and monotonously decreases, which means that the loop nucleation is barrier-less and energetically favorable. It is worth noting that the function $\Delta w(\xi)$ does not in practice depend on the normalized thickness λ of the fiber wall at such a small value of Γ. If $\Gamma \geqslant 1$, growth of λ slightly increases the values of $\Delta w(\xi)$, which leads to an increase in τ_c.

Let us consider the dependence of τ_c on Γ and λ in more detail. It is natural to require that the following conditions be satisfied: $\Delta w(\xi = 1) \leqslant 0$, $\partial \Delta w/\partial \xi|_{\xi=1} = 0$ and $\partial^2 \Delta w/\partial \xi^2|_{\xi=1} < 0$. The first of these conditions guarantees that the loop nucleation is energetically neutral or favorable, the second and third mean that it is in addition barrier-less (see the curve corresponding to $\tau = 1.1D_1$ in Fig. 2). With Eq. (3), these conditions are rewritten as

$$\begin{cases} \tau \geqslant \frac{D_1}{2}\left[1 + [\Gamma + \pi(1-\nu_2)(1-\alpha)]\frac{1-\nu_1}{1-\nu_2}\right] = \tau', \\ \tau = 2D_1\left[2 - A - B + \int_0^{+\infty} \sin\eta f(\eta,\lambda,A,B)\mathrm{d}\eta\right] = \tau'', \\ \left.\frac{\partial^2 \Delta w}{\partial \xi^2}\right|_{\xi=1} = -4(2-A-B) + 4\int_0^{+\infty} \eta\cos\eta f(\eta,\lambda,A,B)\mathrm{d}\eta < 0, \end{cases} \tag{4}$$

respectively. We have analyzed this system numerically and found that the third inequality is valid for any Γ and λ. The right-hand parts of the first and second relations, which are denoted τ' and τ'', are shown in Figure 3 as functions of Γ plotted for different values of λ at $\alpha = 0.5$ and $\nu_1 = \nu_2 = 0.3$. It can be seen from Figure 3 that the straight line $\tau'(\Gamma)$ twice intersects the curve $\tau''(\Gamma)$, in the ranges of small and large values of Γ, thus separating the areas of Γ where the critical stress τ_c should be the larger of τ' and τ'': $\tau_c(\Gamma,\lambda) = \max\{\tau'(\Gamma), \tau''(\Gamma,\lambda)\}$. For example, at $\lambda = 5$, the intersection points are Γ_{c1} (Fig. 3a) and Γ_{c2} (Fig. 3b). In the intervals $0 < \Gamma \leqslant \Gamma_{c1}$ and $\Gamma \geqslant \Gamma_{c2}$, the inequality $\tau' \geqslant \tau''$ is

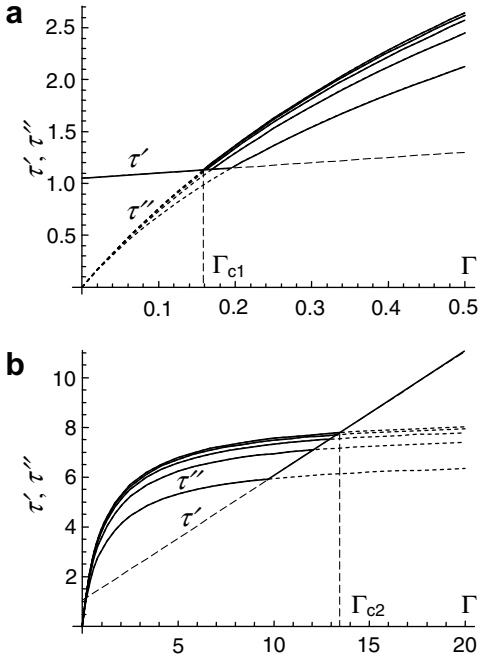

Figure 3. Dependence of the stresses τ' and τ'' on the ratio Γ for different values of $\lambda = 1$, 2, 3, 4 and 5 (from bottom to top) in the field of (a) small and (b) large values of Γ. The solid curves correspond to the critical stress $\tau_c = \max\{\tau', \tau''\}$. The stress values are given in units of D_1.

valid. Therefore, for $\tau \geqslant \tau_c = \tau'$, the loop nucleation is barrier-less and does not lead to the energy increase. If $\Gamma_{c1} < \Gamma < \Gamma_{c2}$, then $\tau'' > \tau'$ and hence at $\tau \geqslant \tau_c = \tau''$, the loop nucleation is energetically favorable and also barrier-less. From Figure 3, we can also conclude that the critical stress τ_c does not depend on the normalized thickness of the fiber wall λ at small and large values of the ratio Γ, and weakly depends on Γ at its medium values. The interval of Γ, in which τ_c depends on λ, increases with increasing λ from approximately $0.2 < \Gamma < 9.3$ at $\lambda = 1$ to $0.16 < \Gamma < 13.5$ at $\lambda = 5$. Of course, these conclusions are valid until our model is correct, i.e. for thin-wall fibers ($\lambda \ll a/b$).

From the practical viewpoint, the most interesting is the area $\Gamma < 1$ because one normally uses fibers that are elastically harder then the ceramic matrix. For $\Gamma < \Gamma_{c1}$ with $\tau_c = \tau'(\Gamma,\alpha)$, one can estimate the smallest possible value of τ_c. Let us neglect the variations in the Poisson ratios and take $\nu_1 = \nu_2 = \nu$. Then the critical stress τ_c is given by

$$\tau_c(\Gamma < \Gamma_{c1}, \nu_1 = \nu_2 = \nu) = \frac{D_1}{2}[1 + \Gamma + \pi(1-\nu)(1-\alpha)]. \tag{5}$$

If the specific interface energy is very large and close to the specific energy of the fiber free surface ($\alpha \to 1$), then neglecting Γ in comparison with 1, we obtain the smallest estimate $\tau_{c,\min} \approx D_1/2 = G_1/[8\pi(1-\nu)]$, which gives $\approx G_1/18$ at $\nu = 0.3$. For the former value $\alpha \approx 0.5$, we have $\tau_c \approx D_1 = G_1/[4\pi(1-\nu)]$, i.e. $\approx G_1/9$. As a result, we can conclude that, for $\Gamma < \Gamma_{c1}$ and $\nu = 0.3$, the critical stress τ_c varies from $\approx G_1/18$ to $\approx G_1/9$.

It seems that such high values of τ_c are overestimated due to the very rough approximations used for the core and surface energy terms. Indeed, we took a standard estimate for the core energy of an edge dislocation in an infinite medium [20,21] although near the free surfaces of the crack and fiber (here at $\xi = 1$), the core energy must be much lower. In a similar way, we used a standard estimate $G_1 b/8$ for the fiber free surface energy. Thus, the estimates obtained may be considered as the upper limits for the critical stress τ_c.

In general, as shown by detailed atomic simulations of various metal–ceramic interfaces [18,22], the Burgers vector of an interface dislocation depends on the ratio between the elastic constants of the materials in contact. Within our model, we have not considered this dependence, because it does not influence results of our calculations operating with dimensionless normalized quantities (see Eqs. (3) and (4), and Figs. 2 and 3).

In summary, we have proposed a dislocation model to describe the glide of hollow fibers as a mechanism of energy relaxation at the bridging stage of fracture in ceramic nanocomposites. Within the model, the fiber glide occurs through generation and slip of prismatic dislocation loops from the crack surface along the fiber–matrix interface. It is shown that these processes can be energetically favorable and barrier-less under high but still real local shear stress acting in the interface near the crack surface. The critical stress value increases as the ratio of the matrix and fiber shear moduli increases. For a wide range of values of this ratio, it also grows with the thickness of the fiber wall. The dislocation mechanism provides significant relaxation of the strain energy near the cracks in ceramic nanocomposites and therefore can increase their toughness.

The work was supported, in part, by the Russian Federal Agency of Science and Innovations (Contract 02.513.11.3190), the Russian Foundation of Basic Research (Grants 08-01-00225-a and 08-02-00304-a) and the National Science Foundation Grant CMMI #0700272.

[1] J.A. Vreeling, V. Ocelik, G.A. Hamstra, Y.T. Pei, J.Th.M. De Hosson, Scripta Mater. 42 (2000) 589.
[2] G.-D. Zhan, J.D. Kuntz, J. Wan, A.K. Mukherjee, Nature Mater. 2 (2002) 38.
[3] S. Veprek, Rev. Adv. Mater. Sci. 5 (2003) 6.
[4] G.-D. Zhan, J.D. Kuntz, A.K. Mukherjee, MRS Bull. 29 (2004) 22.
[5] G.-D. Zhan, J.D. Kuntz, A.K. Mukherjee, Int. J. Appl. Ceram. Technol. 1 (2004) 161.
[6] G.-D. Zhan, A.K. Mukherjee, Rev. Adv. Mater. Sci. 10 (2005) 185.
[7] S. Zhang, D. Sun, Y. Fu, Y.T. Pei, J.Th.M. De Hosson, Surf. Coat. Technol. 200 (2005) 1530.
[8] D. Galvan, Y.T. Pei, J.Th.M. De Hosson, Surf. Coat. Technol. 200 (2005) 6718.
[9] J. Wan, R.-G. Duan, M.J. Gasch, A.K. Mukherjee, J. Am. Ceram. Soc. 89 (2006) 274.
[10] C.C. Koch, I.A. Ovid'ko, S. Seal, S. Veprek, Structural Nanocrystalline Materials: Fundamentals and Applications, Cambridge University Press, Cambridge, 2007.
[11] D.B. Marshall, B.N. Cox, A.G. Evans, Acta Metall. 33 (1985) 2013.
[12] S. Nemat-Nasser, M. Hori, Mech. Mater. 6 (1987) 245.
[13] N.A. Grekov, N.F. Morozov, J. Appl. Math. Mech. 70 (2006) 945.
[14] K.G. Dassios, C. Galiotis, V. Kostopoulos, M. Steen, Acta Mater. 51 (2003) 5359.
[15] K.G. Dassios, V. Kostopoulos, M. Steen, Acta Mater. 55 (2007) 83.
[16] A.G. Evans, D.B. Marshall, Acta Metall. 37 (1989) 2567.
[17] L.S. Sigl, A.G. Evans, Mech. Mater. 8 (1989) 1.
[18] W.P. Vellinga, J.Th.M. De Hosson, V. Vitek, Acta Mater. 45 (1997) 1525.
[19] M.Yu. Gutkin, A.E. Romanov, Edge dislocations in thin inhomogeneous plates, Preprint No. 1407 of the Ioffe Physico-Technical Institute, Leningrad, 1989 (in Russian).
[20] M.Yu. Gutkin, A.E. Romanov, Phys. Stat. Sol. (a) 125 (1991) 107.
[21] J.P. Hirth, J. Lothe, Theory of Dislocations, Wiley, NY, 1982.
[22] J.Th.M. De Hosson, H.B. Groen, B.J. Kooi, V. Vitek, Acta Mater. 47 (1999) 4077.